Progress In Electromagnetics Research Letters, Vol. 92, 9–16, 2020

Design of a 3-D Tunable Band-Stop Frequency Selective Surface with Wide Tuning Range

Shengli Jia[1, 2, *], Bingzheng Xu[1], and Ting Zheng[1]

Abstract—In this paper, a three-dimensional (3-D) tunable band-stop frequency selective surface (FSS) with wide tuning range is presented. The proposed tunable 3-D FSS consists of a periodic array of an annular resonator loaded with two varactor diodes. By controlling the reverse voltage of the varactor diodes, the resonance frequency could be tuned in a wide frequency range. Full-wave simulation shows 100% tuning range from 3.0 GHz to 6.0 GHz with respect to lower resonance frequency. The simulated results exhibit stable band-stop performance under different incident angles (up to 45°). By cascaded two 3-D tunable FSSs, the bandwidth and selectivity performance could be further enhanced. The proposed 3-D FSS with its stable stop-band performance can be a potential candidate to shield the RF signals which is the major source of problem leading to RF device malfunctions.

1. INTRODUCTION

In the last decades, frequency selective surfaces (FSS) have been drawing attention by their special property of selectivity of the frequencies and polarizations of the incident wave. The band-pass or band-stop characteristic of the FSS could be determined by the geometry structure, size, and arrangement of the unit cell [1]. Therefore, FSSs are widely used in radomes, shielding, polarizer, antenna beam steering applications, dichroic reflector, etc. [2, 3].

The latest trend of research on FSS technology is to realize various frequency responses without modifying the geometry of FSS unit cell. By loading with active semiconductor devices like varactor diodes, Pin or Schottky diodes in the element design, the transmission or reflection feature of FSS could be tuned by varying the DC Voltage across the varactor diodes [4–10]. Electronic tunable FSSs have been widely studied in the past few years due to their advantages of small size, nanosecond tuning speed, and low cost.

In recent years, three-dimensional (3-D) FSS has attracted much attention due to its advantages of small size and stable frequency response to different incident wave angles. With compact size and high performance, this new approach may offer an attractive alternative over two-dimensional (2-D) FSSs. In [11], a compact and single layer UWB band-stop FSS was presented to provide electromagnetic shielding for RF signals. A novel 3-D FSS, exhibiting band-pass filtering response with high frequency selectivity, is presented [12]. The 3-D FSS with cylindrical resonator elements was demonstrated offering great flexibility in terms of controlling the frequency response. Although the proposed 3-D FSS shows outstanding performance in many respects [13–18], the research in the field of band-stop FSS with especially high selectivity and small size has not been reported a lot.

In this paper, a 3-D tunable FSS composed of an annular resonator loaded with two varactor diodes is proposed. By altering the values of the added DC voltage, the varactor's capacitance will change and bring the variation of the working frequency realizing the tunability. The simulated results show

Received 19 April 2020, Accepted 4 June 2020, Scheduled 9 June 2020

* Corresponding author: Shengli Jia (jiashengli5@nuaa.edu.cn).

[1] AVIC LeiHua Electronic Technology Research Institute, Wuxi, China. [2] School of Information Science and Engineering, Southeast University, Nanjing, China.

that the proposed tunable FSS has sensitive response when capacitance changes in a certain range. The simulated results exhibit stable band-stop performance under different incident angles (up to 45°) with high selectivity. The bandwidth and selectivity can be further enhanced by cascading two 3-D FSS unit cells.

2. THE 3-D TUNABLE FSS

The structure of the proposed 3-D tunable band-stop FSS is illustrated in Figure 1. The overall dimension of the 3-D FSS unit cell is 3 mm × 5 mm × 6 mm, approximately $0.06\lambda_0 \times 0.1\lambda_0 \times 0.12\lambda_0$, and λ_0 refers to the resonant wavelength at 6.0 GHz in free space. The substrate used for the FSS is Rogers 5880 with permittivity ε_r of 2.2, loss tangent of 0.009, and thickness of 1 mm. A foam substrate which has permittivity ε_r of 1.04, loss tangent of 0.009, and thickness of 4 mm is used to separate the adjacent unit cells along x direction. The annular resonator is composed of two microstrip lines and two metal vias. Two varactor diodes are loaded in the middle of the microstrip lines, respectively. The diode selected in this work is the Skyworks SMV1405-074LF, which has a nominal zero-bias junction capacitance between 0.3 and 1.3 pF. The parameters for the final layout of the proposed tunable FSS are as follows: $L = 4.8$ mm, $W = 0.5$ mm, $S = 0.2$ mm.

To investigate the characteristics of the proposed tunable FSS, a full-wave EM field solver CST-MWS is used to simulate the transmission and reflection coefficient of the proposed FSS when being illuminated by x-polarized plane waves. The incident x-polarized plane wave propagates along $+Z$

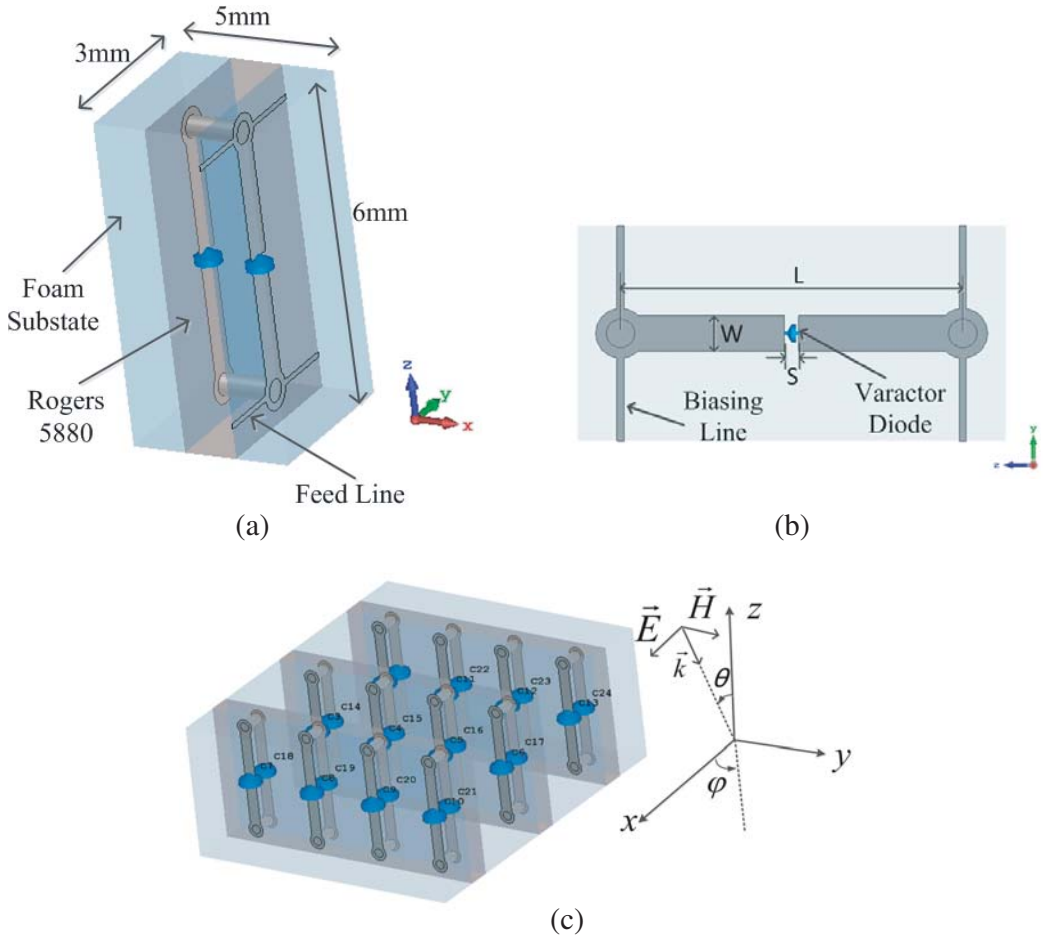

Figure 1. Structure of the proposed tunable 3-D band-stop FSS. (a) Unit cell. (b) Side view of the unit cell. (c) Perspective view of the FSS array.

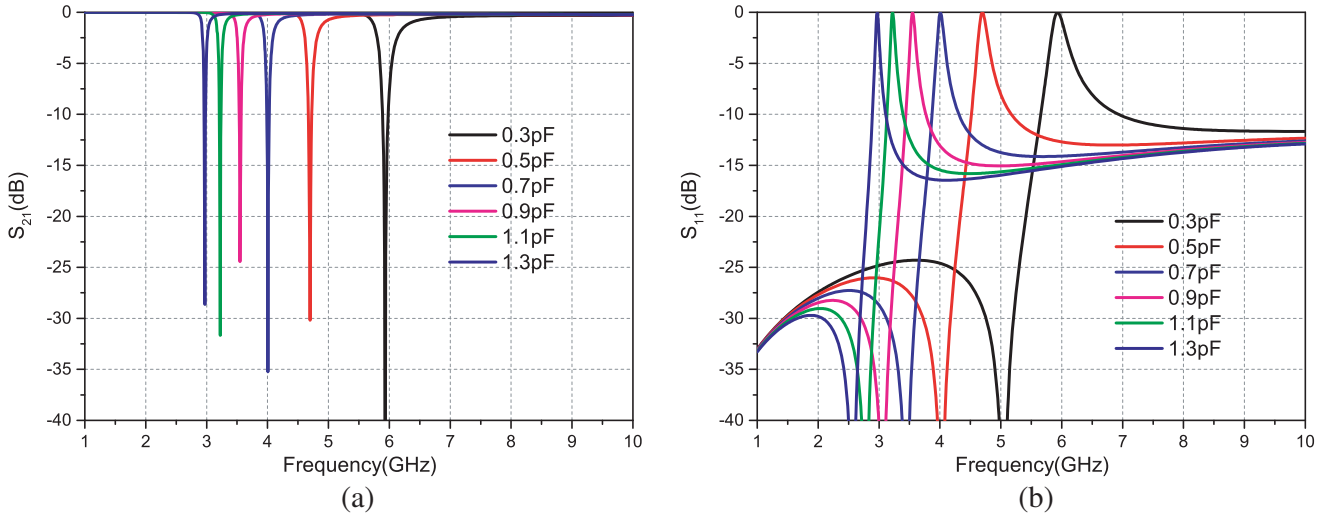

Figure 2. Simulated transmission and reflection coefficient of the proposed 3-D tunable FSS. (a) S_{21}. (b) S_{11}.

direction. The unit cell boundary condition and Floquet ports are applied to imitate the infinite FSS.

By controlling the DC voltage across the varactor diodes, the varactor's capacitance will change, and the resonant frequency of the band-stop FSS can be tuned in a wide frequency range. Figure 2 shows the simulated transmission and reflection coefficients of the proposed 3-D tunable FSS. It is obvious that the working frequency decreases when the capacitance is increased. The center frequency varies from 3.0 GHz to 6.0 GHz, which corresponds to the capacitance of 0.3 pF to 1.3 pF. Hence, the tunable range is nearly 100% with reference to the lower frequency and 66.7% with respect to the center frequency. The proposed FSS is able to produce a narrow stop-band with high selectivity. In the case of 0.5 pF-capacitance, the half (−3 dB) bandwidth is about 3.8% (from 4.62 GHz to 4.8 GHz). A reflection zero appears below the stop-band under perpendicular incident wave, and excellent filtering performance could be obtained compared to the traditional 2-D FSSs.

To investigate the operating mechanism of the 3-D band-stop FSS, the current distributions at different frequencies on the annual resonator are plotted in Figure 3. The surface current is plotted at 4.0 GHz, 4.7 GHz, and 6.0 GHz for a diode capacitance of 0.5 pF. Analyzing the results in Figure 3, it is seen that the surface current at 4.7 GHz is stronger than the other frequency points, i.e., the incident x-polarized wave excites ring current along the annular resonator at 4.7 GHz, and a transmission null occurs. Thus the stop-band frequency changes when the resonant frequency of the annual resonator changes. Therefore, the stop-band frequency could be controlled by changing the varactor capacitance.

Angular stability refers to a phenomenon in which the frequency response of the FSS remains unchanged by variation in the incident angle of the incoming electromagnetic wave. The miniaturization of the structural unit improves the angular stability performance of the 3-D FSS as the phase variation is small over the structure whose dimensions are less. Figure 4 shows the simulated transmission and reflection coefficients of the proposed 3-D FSS under different incident angles. The capacitances of the varactor diodes are fixed to 0.5 pF, and the center frequency of the band-stop FSS is about 4.7 GHz. It shows almost stable responses for 0° to 45° with a step of 15°. It is clearly seen that the stop-band performance of the proposed 3-D FSS is extremely stable with respect to different incident angles. What needs to be emphasized is that the angular stability performance is stable when the capacitances of the varactor diodes change from 0.3 pF to 1.3 pF, but only the simulated results of 0.5 pF-capacitance are included in this paper to keep the paper reasonably concise.

3. DESIGN OF THE CASCADED 3-D TUNABLE FSS

To overcome the drawback of the narrow bandwidth performance, two 3-D FSS unit cells are cascaded along Z-axis to form a new cascaded 3-D tunable FSS. Figure 5 shows the geometry of the cascade 3-D

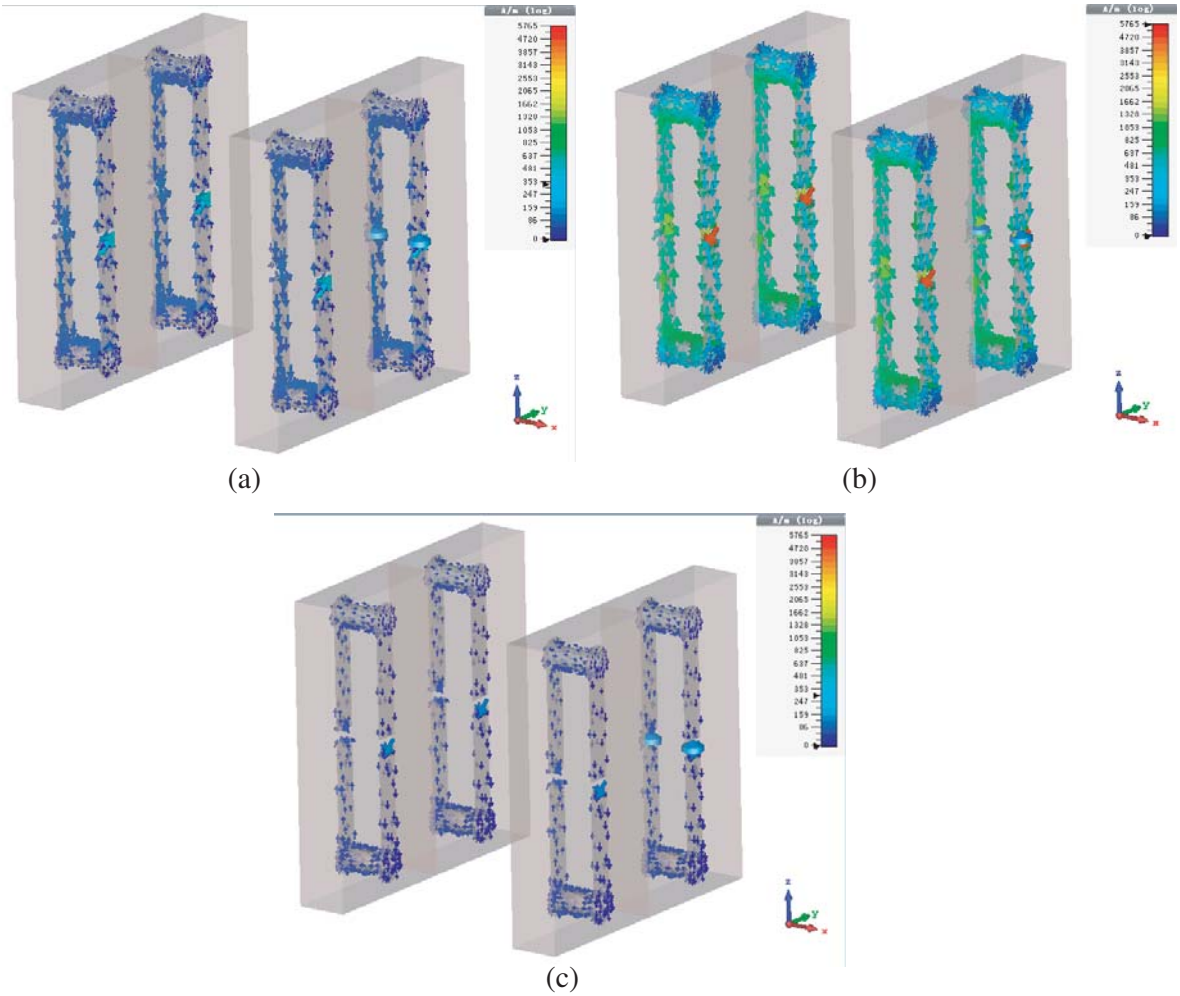

Figure 3. The current distribution on the surface of the annual resonator. (a) 4.0 GHz. (b) 4.7 GHz. (c) 6.0 GHz.

Table 1. Comparison with other tunable band-stop FSS.

FSS structure	Configuration	Size	Tunable range (GHz)	Angular stability
[5]	2-D with Varactor diode	$0.306\lambda_0 \times 0.306\lambda_0 \times 0.006\lambda_0$	8.33 to 9.17	Not reported
[6]	2-D with Varactor diode	$0.41\lambda_0 \times 0.41\lambda_0 \times 0.027\lambda_0$	3.5 to 8.2	Not reported
[7]	2-D with Varactor diode	$0.15\lambda_0 \times 0.15\lambda_0 \times 0.09\lambda_0$	2.67 to 3.52	Not reported
[8]	2-D with Varactor diode	$0.38\lambda_0 \times 0.38\lambda_0 \times 0.015\lambda_0$	3.4 to 3.8	Not reported
This work	3-D with Varactor diode	$0.06\lambda_0 \times 0.1\lambda_0 \times 0.12\lambda_0$	3.0 to 6.0	45°

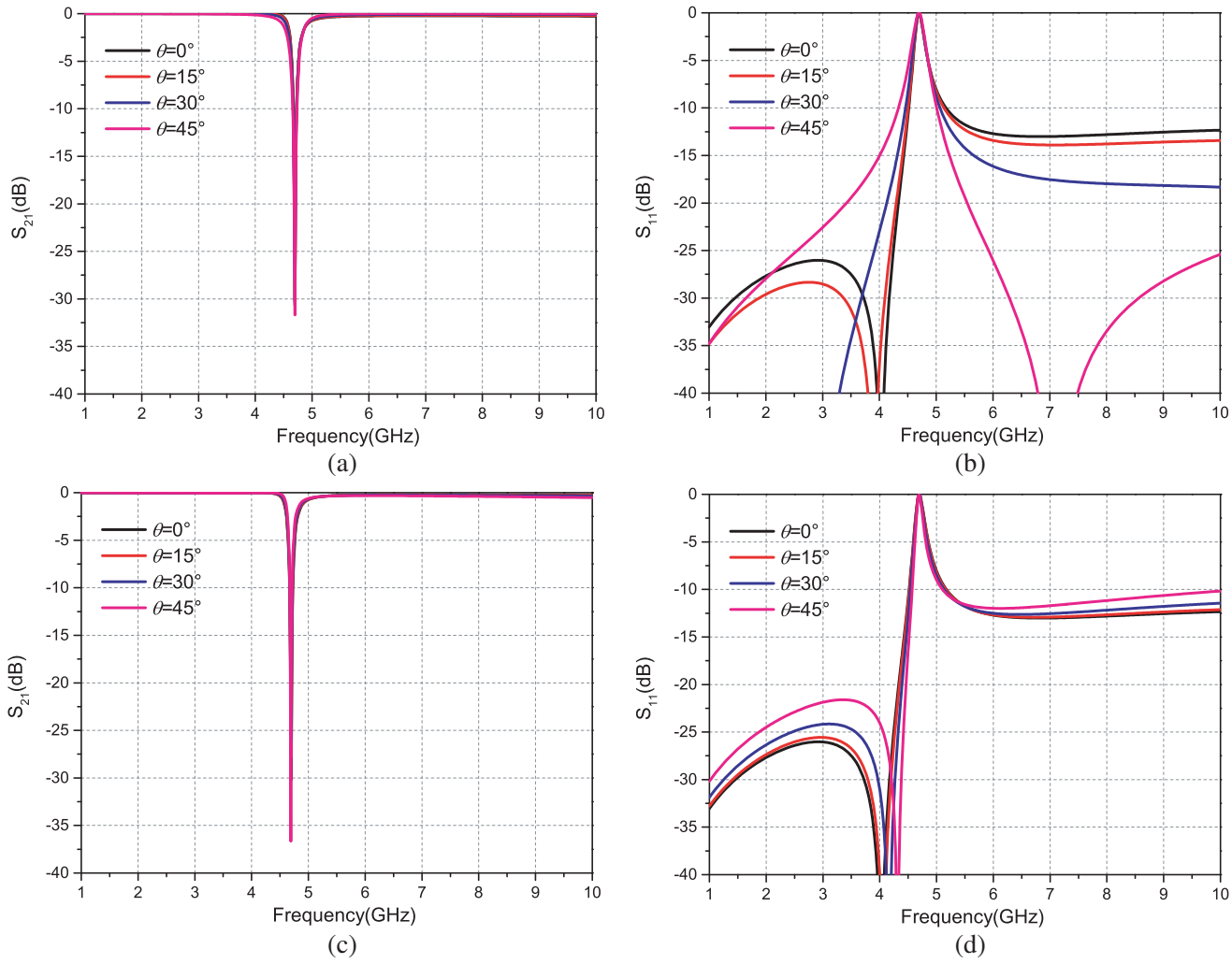

Figure 4. Simulated transmission and reflection coefficient of the proposed 3-D FSS for different incident angle. (a) S_{21}, $\varphi = 0°$. (b) S_{11}, $\varphi = 0°$. (c) S_{21}, $\varphi = 90°$. (d) S_{11}, $\varphi = 90°$.

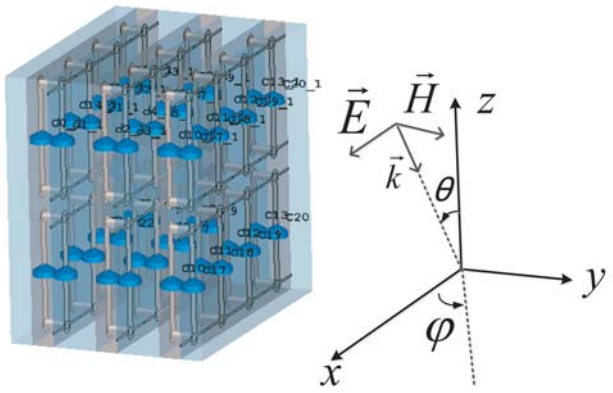

Figure 5. Geometry of cascaded 3-D tunable FSS.

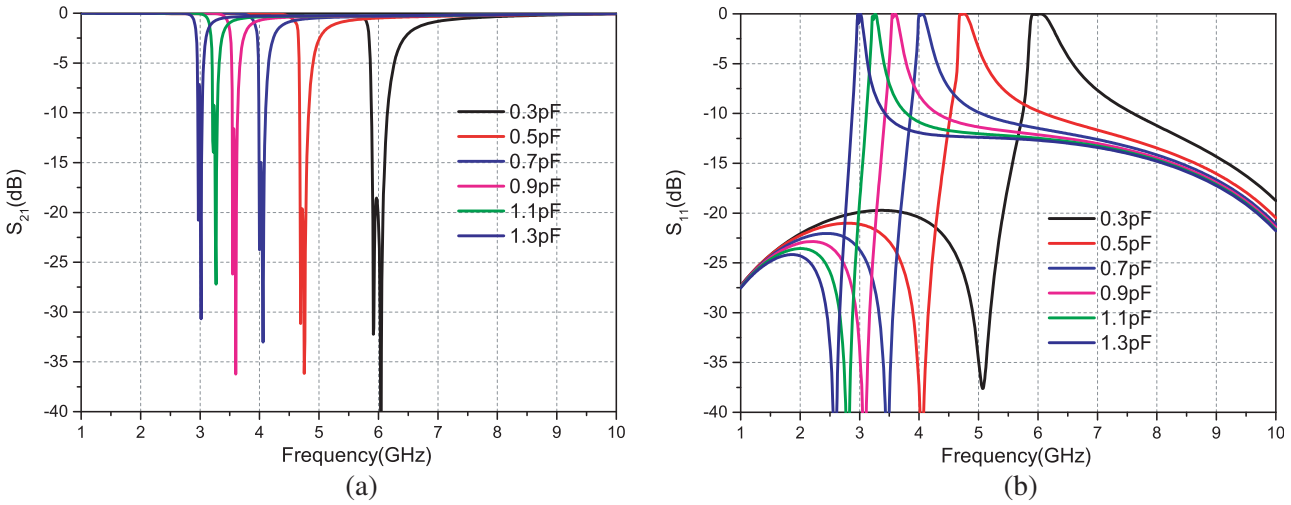

Figure 6. Simulated transmission and reflection coefficient of the cascaded 3-D tunable FSS. (a) S_{21}. (b) S_{11}.

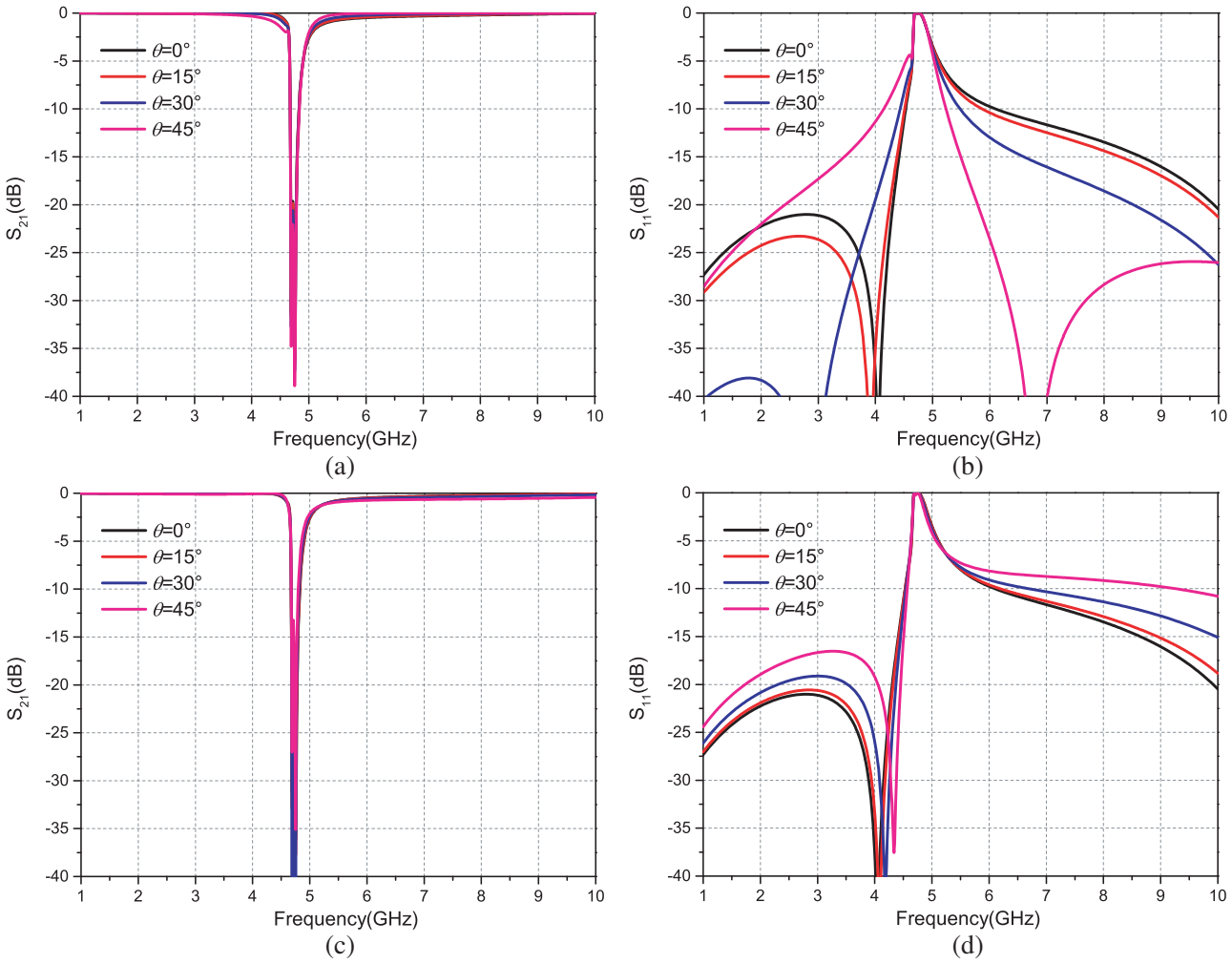

Figure 7. Simulated transmission and reflection coefficient of the cascaded 3-D tunable FSS for different incident angle. (a) S_{21}, $\varphi = 0°$. (b) S_{11}, $\varphi = 0°$. (c) S_{21}, $\varphi = 90°$. (d) S_{11}, $\varphi = 90°$.

tunable FSS. The varactor diodes loaded in the annular resonator have the same DC Voltage in both FSS unit cells which leads to the same capacitance. The length of the annular resonator is $L1 = 4.6\,\text{mm}$ and $L2 = 4.8\,\text{mm}$.

Figure 6 shows the simulated transmission and reflection coefficients of the cascaded 3-D FSS with different capacitance values. The center frequency varies from 3.0 GHz to 6.0 GHz, which corresponds to the capacitance of 0.3 pF to 1.3 pF same as the single layer 3-D FSS. In the case of 0.5 pF-capacitance, the half ($-3\,\text{dB}$) bandwidth is about 7.3% (from 4.65 GHz to 5.0 GHz). It is obvious that the bandwidth of the cascaded 3-D FSS is broadened compared to the single-layer 3-D FSS. It could be seen that two transmission zeros appear in the stop-band which enhance the bandwidth of the cascaded 3-D tunable FSS remarkably. And the selectivity of the FSS maintains well while the working frequency changes.

Figure 7 shows the simulated transmission coefficients of the cascaded 3-D tunable FSS under different incident angles. It is clearly seen that the bandwidth and in-band performance are almost unchanged when the incident angle increases. The out-of-band performance of the cascaded 3-D FSS maintains well when the incident angle increases to 45°. The simulated results demonstrate that the cascaded two-layer 3-D FSS has wider stop-band bandwidth and better out-of-band performance than the single-layer 3-D FSS.

Performance comparison of the proposed 3-D tunable band-stop FSS and other FSSs available in the literature is illustrated in Table 1. From the above table, it is evident that the proposed 3-D tunable band-stop FSS offers compact size and good angular stability compared to the other tuning techniques reported in the literature.

4. CONCLUSION

In this paper, the design of a 3-D tunable band-stop FSS with wide tuning range is presented. By altering the DC voltage across the varactor diodes loaded in the annular resonator, the working frequency of the FSS shifts significantly. Simulated results show that tunable frequency range is more than 100% with respect to the lower resonance frequency, demonstrating a wide tuning range. The simulated results also show that the designed 3-D FSS exhibits high selectivity at different angles of incidence (up to 45°). By cascading two 3-D tunable FSS unit cells, the stop-band bandwidth and selectivity performance could be further enhanced. The proposed 3-D tunable band-stop FSS shows wide tuning rang and good angular stability, with many potential applications in the electromagnetic shielding field.

ACKNOWLEDGMENT

This work has been funded by China Postdoctoral Science Foundation (2019M651992).

REFERENCES

1. Munk, B. A., *Frequency Selective Surfaces: Theory and Design*, Wiley, New York, USA, 2000.
2. Yu, Y. M., C. N. Chiu, Y. P. Chiou, and T. L. Wu, "An effective via-based frequency adjustment and minimization methodology for single-layered frequency-selective surfaces," *IEEE Transactions on Antennas and Propagation*, Vol. 63, No. 4, 1061–1049, 2015.
3. Liu, N., X. J. Sheng, and J. J. Fan, "A compact miniaturized frequency selective surface with stable resonant frequency," *Progress in Electromagnetic Research Letters*, Vol. 62, 17–22, 2016.
4. Mias, C. and J. H. Yap, "A varactor-tunable high impedance surface with a resistive-lumped-element biasing grid," *IEEE Trans. Antennas Propag*, Vol. 55, No. 7, 1955–1962, 2007.
5. Vez, F. J. L., J. Rodriguez-Cuevas, A. E. Martynyuk, and J. I. Martinez-Lopez, "Active frequency selective surfaces based on loaded ring patches," *2018 IEEE International Conference on Computational Electromagnetics*, 1–2, 2018.
6. Sivasamy, R., B. Moorthy, and M. Kanagasabai, "A wideband frequency tunable FSS for electromagnetic shielding applications," *IEEE Trans. on Electromagnetic Compatibility*, Vol. 60, 280–283, 2018.

7. Withayachumnankul, W., C. Fumeaux, and D. Abbott, "Planar array of electric-LC resonators with broadband tunability," *Antennas and Wireless Propagation Letters*, Vol. 10, 557–580, 2011.
8. Neto, A. G., J. C. e Silva, A. G. Barboza, D. F. Mamedes, I. B. G. Coutinho, and M. de Oliveira Alencar, "Varactor-tunable four arms star bandstop FSS with a very simple bias circuit," *2019 13th European Conference on Antennas and Propagation (EuCAP)*, 1–5, 2019.
9. Mamedes, D. F., A. Gomes Neto, J. C. e Silva, and J. Bornemann, "Design of reconfigurable frequency-selective surfaces including the PIN diode threshold region," *IET Microwaves, Antennas and Propagation*, Vol. 12, No. 9, 1483–1486, 2018.
10. Azemi, S. N., K. Ghorbani, and W. S. T. Rowe, "A reconfigurable FSS using a spring resonator element," *IEEE Antennas Wireless Propag. Lett*, Vol. 12, 781–784, 2013.
11. Rafique, U. and S. Agarwal, "A modified frequency selective surface band-stop filter for ultra-wideband applications," *2018 International Conference on Advances in Computing, Communications and Informatics (ICACCI)*, 1653–1656, 2018.
12. Tao, K., B. Li, Y. M. Tang, M. Zhang, and Y. M. Bo, "Analysis and implementation of 3D bandpass frequency selective structure with high frequency selectivity," *Electronics Letters*, Vol. 53, No. 5, 324–326, 2017.
13. Azemi, R. S. N. and W. S. T. Rowe, "Development and analysis of 3D frequency selective surfaces," *IEEE Asia-Pacific Microwave Conference Proceedings (APMC)*, 2011.
14. Azemi, S. N., K. Ghorbani, and W. S. T. Rowe, "3D frequency selective surfaces," *IEEE Antennas and Propagation Conference*, 2012.
15. Omar, A. A. and Z. Shen, "Multiband high-order bandstop 3-D frequency-selective structures," *IEEE Transactions on Antennas and Propagation*, Vol. 64, No. 6, 2217–2226, 2016.
16. Li, B. and Z. Shen, "Three-dimensional bandpass frequency-selective structure with multiple transmission zeros," *IEEE Trans. Microw. Theory Tech*, Vol. 61, No. 10, 3578–3589, 2013.
17. Kanth, V. K. and S. Raghavan, "3D frequency selective surfaces based on substrate integrated waveguide technology," *2018 IEEE MTT-S International Microwave and RF Conference (IMaRC)*, 2018.
18. Yu, W., G. Q. Luo, Y. Yu, Z. Liao, H. Jin, and Z. Shen, "Broadband band-absorptive frequency-selective rasorber with a hybrid 2-D and 3-D structure," *IEEE Antennas and Wireless Propagation Letters*, Vol. 8, No. 18, 1701–1705, 2019.